The Journal of Experimental Biology 210, 2912-2922
Published by The Company of Biologists 2007
doi:10.1242/jeb.006874

Sensory-induced modification of two motor patterns in the crab, *Cancer pagurus*

Carmen R. Smarandache and Wolfgang Stein*
Institute of Neurobiology, Ulm University, D-89069 Ulm, Germany
*Author for correspondence (e-mail: wstein@neurobiologie.de)

Accepted 16 May 2007

Summary

Sensory input is pervasive among motor networks and continuously adapts motor patterns to changing circumstances. To elucidate common principles of sensorimotor integration, it is beneficial to characterize sensory influences on motor network operation and compare these influences between species. To facilitate such comparison, we have studied the influence of the anterior gastric receptor (AGR) – a proprioceptor that has been characterized in detail in two lobster species – on the pyloric (filtering of food) and gastric mill (chewing of food) motor patterns in the crab *Cancer pagurus*.

AGR has a bipolar cell body in the stomatogastric ganglion; it was activated by tension increase in gastric mill powerstroke muscles. While two spike initiation zones accounted for its spontaneous activity, active membrane properties (sag potentials, spike frequency adaptation) contributed to the AGR response to current injections.

When activated, AGR diminished spike activities in two pyloric motor neurons and prolonged the pyloric cycle period. Furthermore, AGR excited gastric mill protractor neurons, inhibited the retractor neuron and evoked phase-independent resetting of the gastric mill rhythm. Repetitive spike trains entrained the rhythm to both longer and shorter cycle periods. All AGR actions seemed to be mediated *via* at least two premotor projection neurons in the spatially distant commissural ganglia. The response of the gastric mill neurons was independent of AGR firing frequency.

Our results suggest that homologous proprioceptors can elicit similar effects on motor patterns while utilizing different mechanisms. This work thus provides an initial framework for future studies to determine underlying common principles.

Key words: *Cancer pagurus*, stomatogastric ganglion, projection neuron, central pattern generation, sensory regulation.

Introduction

Sensory feedback to motor networks ensures proper motor output so that the resulting behavior is continuously adapted to changing circumstances. In rhythmically active networks, proprioceptive and mechanosensory feedback is often coordinated with the activity of central pattern generators (CPGs) and reorganizes their functioning (Beenhakker and Nusbaum, 2004; Büschges, 2005; Cropper et al., 2004; Perrins et al., 2002).

While the effects of sensory regulation on the nervous systems are well known in many organisms, a comparison of the effects of homologous sensory systems in different, but related, species has rarely been investigated (e.g. Wolf et al., 2001). For example, are the effects of a sensory organ on motor output species-specific or a more general aspect of sensory feedback? There are few systems for which detailed information on the functional characteristics of circuit neurons and the motor output is available to support such investigation. One such system is the stomatogastric nervous system (STNS) of decapod crustaceans, which has been characterized in several different crustaceans (Marder and Bucher, 2001; Nusbaum and Beenhakker, 2002; Selverston and Moulins, 1987). The STNS is an extension of the central nervous system, which contains two CPGs that control the movement of food throughout the foregut. While the gastric mill circuit generates the motor output responsible for the chewing movement of three internal teeth (two lateral and one medial), the pyloric pattern generator drives the rhythmic movements of the pyloric filter apparatus (Hartline and Maynard, 1975; Maynard and Dando, 1974). The circuitries of the gastric mill and pyloric CPGs are located in the stomatogastric ganglion (STG) and have extensively been characterized in several crustacean species.

A proprioceptor that is particularly suited for investigating the effects of sensory feedback on the STG circuits is the anterior gastric receptor (AGR), which was initially described in the crayfish (Larimer and Kennedy, 1966) and then characterized in detail in the European lobster *Homarus gammarus* (Combes et al., 1995; Combes et al., 1997; Combes et al., 1999; Simmers and Moulins, 1988a; Simmers and Moulins, 1988b) and the spiny lobster *Panulirus interruptus* (Elson et al., 1994). In both lobster species AGR occurs as a single bipolar cell body in the STG and measures the tension of the muscles responsible for protraction of the medial tooth. Its function is thus comparable to that of vertebrate Golgi tendon organs.

AGR spikes are initiated in its dendrites close to the location where AGR innervates the bilaterally symmetric powerstroke muscles gm1 (Combes et al., 1993). The response of AGR to a tonic tension increase of the gm1 muscles shows no adaptation (Combes et al., 1995). Interestingly, receptor activity can also

be oscillatory, depending on neuromodulatory influences on its dendritic compartment (Combes et al., 1997).

AGR participates in a long-loop reflex pathway; that is, without direct effects on the gastric mill cells in the STG. Rather, it excites premotor descending projection neurons in the commissural ganglia, which, in turn, affect the STG motor neurons (Combes et al., 1999; Elson et al., 1994; Simmers and Moulins, 1988a; Simmers and Moulins, 1988b). As a result, AGR activity can reset and entrain the gastric mill rhythm (Elson et al., 1994). Additionally, the AGR pathway is involved in a complex control of forces exerted during the muscle powerstroke. While the gastric mill neurons receive excitation during moderate AGR firing frequencies, this excitation is either absent or is superimposed by inhibition (Elson et al., 1994) at higher firing frequencies (Simmers and Moulins, 1988b). Consequently, the gastric mill rhythm is reconfigured depending on AGR firing frequency such that low frequencies synchronize the movements of medial and lateral teeth while strong AGR activity causes alternating teeth movements (Combes et al., 1999).

Here, we study AGR in the isolated nervous system of the crab *Cancer pagurus*. For the first time, we characterize its effects on the pyloric rhythm, in addition to its influence on the gastric mill rhythm. While AGR effects on the gastric mill rhythm in *C. pagurus* are similar to those obtained in the lobster – it entrains and resets the gastric mill rhythm – intracellular recordings from AGR reveal that in *C. pagurus*, by contrast to the lobster, AGR possesses active membrane properties such as sag potentials and spike frequency adaptation. Besides, the sign of the response (excitation/inhibition) of the gastric mill neurons is independent of AGR firing frequency. Our results suggest that homologous proprioceptors in different, but related, species regulate motor pattern *via* different mechanisms.

Materials and methods

Animals

Adult crabs (*Cancer pagurus* L.) were purchased from commercial sources (Feinfisch GmbH, Neu-Ulm, Germany). Crabs were maintained in filtered, aerated artificial seawater (10–12°C). Animals were anesthetized by packing them in ice for 20–40 min before dissection. The dissection of the STNS was done in physiological saline at ~4°C as described previously (e.g. Blitz and Nusbaum, 1997). Experiments were performed on the isolated STNS (Fig. 1A). The neurons in the stomatogastric nervous system of *C. pagurus* and their connectivity and properties are similar to those in *Cancer borealis* (Heinzel et al., 1993; Stein et al., 2005; Stein et al., 2006). Experiments were carried out in accordance with the European Communities Council Directive of 24 November 1986 (86/609/EEC) and with the Guidelines laid down by the NIH in the USA regarding the care and use of animals for experimental procedures.

Solutions

C. pagurus physiological saline had the following composition (mmol l^{-1}): NaCl, 440; $MgCl_2$, 26; $CaCl_2$, 13; KCl, 11; Trisma base, 10; maleic acid, 5. In some experiments, high divalent saline ($5\times Ca^{2+}/5\times Mg^{2+}$) was applied exclusively to the STG to block polysynaptic connections. High divalent saline increases spike threshold in STG neurons (M. P. Nusbaum, personal communication) and had the following compositions (mmol l^{-1}): NaCl, 440; $MgCl_2$, 130; $CaCl_2$, 65; KCl, 11; Trisma base, 10; maleic acid, 5. Furthermore, low-calcium saline was used for blocking chemical synapses in the STG [composition (mmol l^{-1}): NaCl, 440; $MgCl_2$, 39; $CaCl_2$, 0.1; KCl, 11; Trisma base, 11.2; maleic acid, 5.1]. All solutions were kept at a constant temperature of 10–13°C and at pH 7.4–7.6. In some experiments, neuropeptide F1 (TNRNFLRFamide; Bachem, Weil am Rhein, Germany) was focally applied to the dendritic region of AGR at a concentration of 10^{-6} mol l^{-1} (diluted in *C. pagurus* saline).

Electrophysiology

Dissections were carried out as described previously (Blitz and Nusbaum, 1997). The STNS was pinned down in a silicone elastomer-lined (ELASTOSIL RT-601; Wacker, Munich, Germany) Petri dish and superfused continuously (7–12 ml min^{-1}) with chilled physiological saline (10–13°C). Standard intracellular and extracellular recording techniques were used in this study (Stein et al., 2005; Stein et al., 2006). Extracellular recordings of neuronal activity were obtained by electrically isolating individual sections of STNS nerves from the bath by building a petroleum-jelly-based cylindrical compartment around a nerve section. The action potentials propagating through the nerve were recorded by placing one of two stainless steel electrode wires within this compartment. The second wire was placed in the bath as a reference electrode. The differential signal was recorded, filtered and amplified through an amplifier (Model 1700; AM Systems, Carlsborg, WA, USA).

In several experiments, the insertions of the gm1 muscles were left attached to the stomach wall and transferred along with the innervating nerves to the Petri dish. The anterior apodemes of the muscles were then pinned down on Sylgard®, and the posterior ossicles into which the muscles insert were either fixed to a clamp for imposing passive stretch or pinned down on Sylgard® for monitoring isometric contractions.

The gastric mill rhythm was monitored by the activity of the lateral gastric (LG; one cell), dorsal gastric (DG; one cell) and gastric mill (GM; four cells) neurons. The gastric mill rhythm was considered spontaneously active when the LG neuron (a member of the gastric mill CPG) produced bursts of spike activity. The gastric mill cycle period was defined as the duration between the onset of an impulse burst in LG and the onset of the subsequent LG burst. LG was recorded extracellularly from the lateral gastric nerve (*lgn*); the DG and GM neurons were recorded extracellularly from the dorsal gastric nerve (*dgn*). AGR activity was assessed with extracellular recordings of the *dgn*, *stn* (stomatogastric nerve) and/or *son* (superior oesophageal nerve) or with intracellular recordings from the AGR cell body. All activities were measured either as the number of action potentials per burst or as the instantaneous firing frequency as determined by interspike interval. Mean values for all gastric mill-related parameters were determined from measurements of 10 consecutive cycles of gastric mill activity.

To facilitate intracellular recordings and access for applied solutions, the STG was desheathed and visualized with white light transmitted through a darkfield condenser (Nikon, Tokyo,

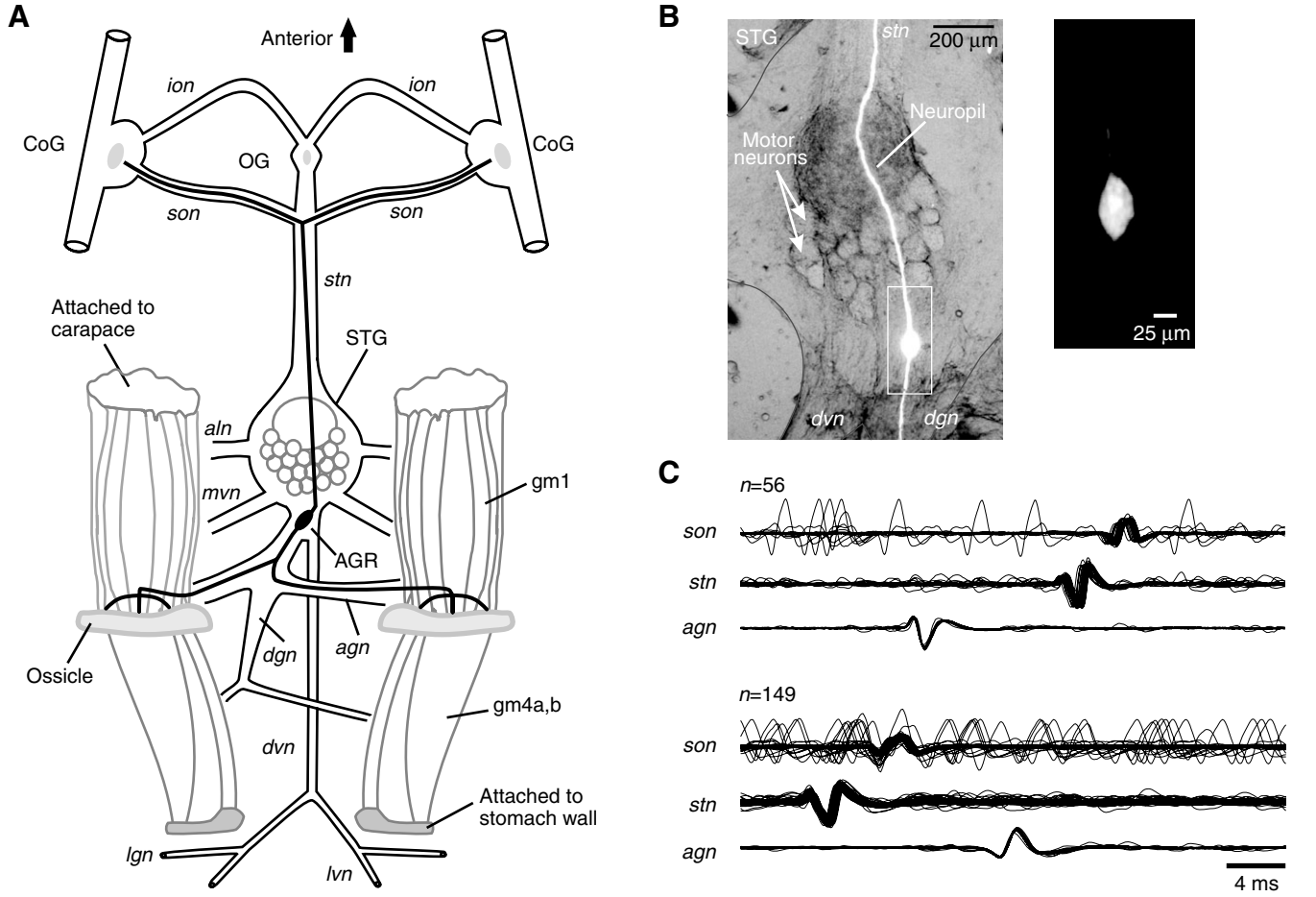

Fig. 1. Morphological and electrophysiological identification of the AGR. (A) Schematic drawing of isolated STNS with gastric muscles gm1 and gm4a,b. The bipolar cell body of the sensory neuron AGR is located immediately posterior to the cell bodies of the motor neurons in the STG and projects one axon *via* the *dgn* and *agn* to the gm1 muscles and one axon *via* the *stn* and *sons* to the CoGs. (B) Lucifer Yellow fill of AGR showing the location of the AGR soma in the STG. AGR possessed no arborization in the STG neuropil. (C) Two spike initiation zones contributed to AGR spontaneous spike activity. Top: multisweep recordings (*n*=56 sweeps) of *agn*, *stn* and *son*, triggered on the AGR action potential on *agn.* The AGR spike could be seen on all recordings. Bottom: 149 sweeps of *agn*, *stn* and *son*, triggered on the AGR action potential on *stn*. CoG, commissural ganglion; OG, oesophageal ganglion; STG, stomatogastric ganglion; AGR, anterior gastric receptor; *agn*, anterior gastric receptor nerve; *aln*, anterior lateral nerve; *dgn*, dorsal gastric nerve; *dvn*, dorsal ventricular nerve; *ion*, inferior oesophageal nerve; *lgn*, lateral gastric nerve; *lvn*, lateral ventricular nerve; *mvn*, median ventricular nerve; *son*, superior oesophageal nerve; *stn*, stomatogastric nerve.

Japan). Microelectrodes (15–25 MΩ) were filled with a solution containing 0.6 mol l^{-1} K_2SO_4 and 0.02 mol l^{-1} KCl. Intracellular current injections were accomplished using NPI NEC 10L (NPI, Tamm, Germany) and Axoclamp 2B amplifiers (Molecular Devices, Sunnyvale, CA, USA) in bridge or single electrode discontinuous current clamp mode. Sample rates in discontinuous current clamp mode ranged from 2 to 4 kHz. Identification of STG neurons was done by assessing their activity patterns, synaptic interactions and axonal projection pathways in combination with current injections, as described previously (Bartos and Nusbaum, 1997; Blitz and Nusbaum, 1997; Weimann et al., 1991).

Data analysis

Data were recorded onto computer hard disk using Spike2 (ver. 5.03–5.14; CED, Cambridge, UK) and a micro 1401 AD board (CED). Data were analyzed with Spike2 script language. Individual scripts are available at http://www.neurobiologie.de/spike2. Final figures were prepared with CorelDraw (version 12.0 for Windows). Graphics and statistics were generated using Excel (Microsoft) or Plotit (version 3.2; Scientific Programming Enterprises, Haslett, MI, USA). Statistical tests for data analysis were Student's *t*-test and paired samples *t*-test. Data are presented as means ± s.d. *N* refers to the number of animals, while *n* gives the number of trials. For all statistical tests, significance with respect to the control was indicated on the figures using the following symbols: $*P<0.05$ and $**P<0.01$.

Nerve backfills and intracellular stainings

To determine the projection pattern of AGR, Lucifer Yellow–CH (LY; Sigma-Aldrich, Munich, Germany) and $NiCl_2$ backfills of the *dgn* were made using standard techniques (e.g.

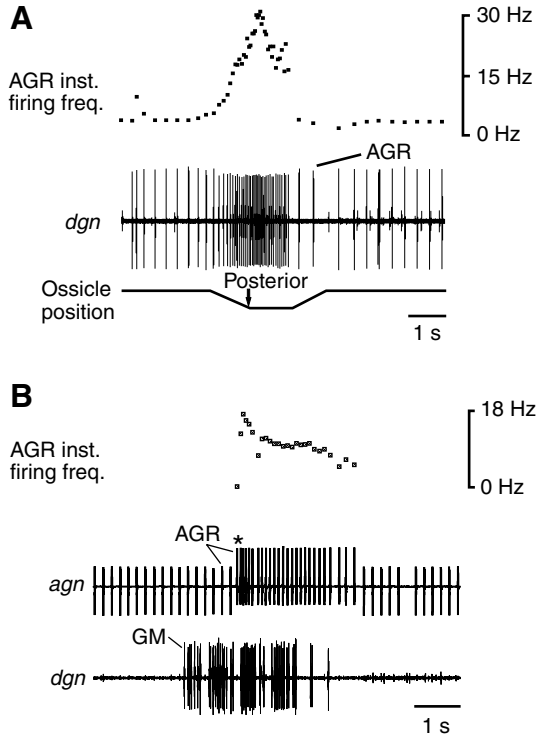

Fig. 2. AGR responds to tension increase in gm1 muscles. (A) Extracellular recording of AGR on *dgn* during passive stretch of a gm1 muscle. Stretch was applied by moving the ossicle between the gm1 and gm4 muscles in the posterior direction. AGR firing frequency increased during the stretch (top trace). (B) Extracellular recording of AGR on *agn* during isometric contraction of a gm1 muscle. Anterior and posterior muscle attachment sites were fixed to the Sylgard® such that the muscle attained its resting length (measured beforehand in the intact animal). During spontaneous gastric mill rhythms, activity of the GM motor neurons (bottom trace) activated AGR. Before GM activity, the AGR spike initiation zone in the *stn* was active. During GM activity, the spike initiation zone close to the muscle became active (*). The top trace shows AGR firing frequency in this condition. See text for definition of abbreviations.

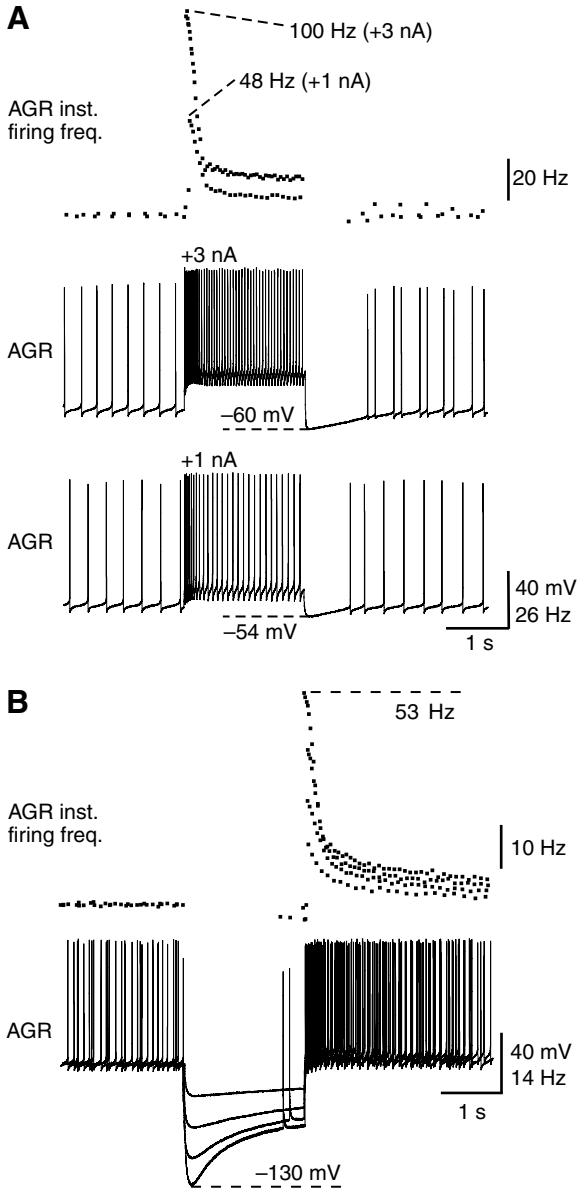

Fig. 3. The anterior gastric receptor (AGR) shows spike frequency adaptation and sag potential. (A) Intracellular recording of AGR. AGR was depolarized with current injections. Bottom, +1 nA; middle, +3 nA; top trace, adaptation of AGR firing frequency during current injections. After an initial peak, firing frequencies dropped to constant value. (B) Current injections were used to hyperpolarize AGR to different membrane potentials. After an early hyperpolarized peak, the membrane potential decayed to a constant value (sag). After the end of the hyperpolarization, the membrane potential transiently overshot the resting potential and AGR firing frequencies increased (top trace).

Coleman et al., 1992; Blitz and Nusbaum, 1999). In these experiments, a Vaseline™ well was built around the *dgn*, and the saline within the well was replaced with distilled water. After several minutes, the distilled water was removed and replaced with a solution of 10% LY or 10% $NiCl_2$ in distilled water; then, the nerve was transected within the well. The preparation was then incubated at 4°C for 18–72 h; the dye was then removed from the well and the preparation fixed and mounted for viewing.

For intracellular stainings, microelectrodes were filled with 1 mol l^{-1} LiCl (shaft solution) and 5% LY (tip solution; tip resistance, 40–70 MΩ). Dye was injected into the AGR cell body by applying 5 nA hyperpolarizing current pulses for 5 s at a rate of 0.15 pulses s^{-1} for about 1 h.

Results

Basic properties of the sensory neuron AGR

Several approaches, including extra- and intracellular electrophysiology (N>50), nerve backfills (N=8) and intracellular stainings of AGR (N=18), were combined to determine the projection pattern of AGR in *C. pagurus*. As previously documented in several crustacean species (Norris et al., 1994; Simmers and Moulins, 1988a; Simmers and Moulins, 1988b), AGR possessed a large bipolar cell body (length 82.0±12.6 μm, width 35.2±5.8 μm; N=6) located at the posterior end of the STG (Fig. 1B). In *C. pagurus*, one of its axons projected posteriorly to the bilaterally symmetric gastric

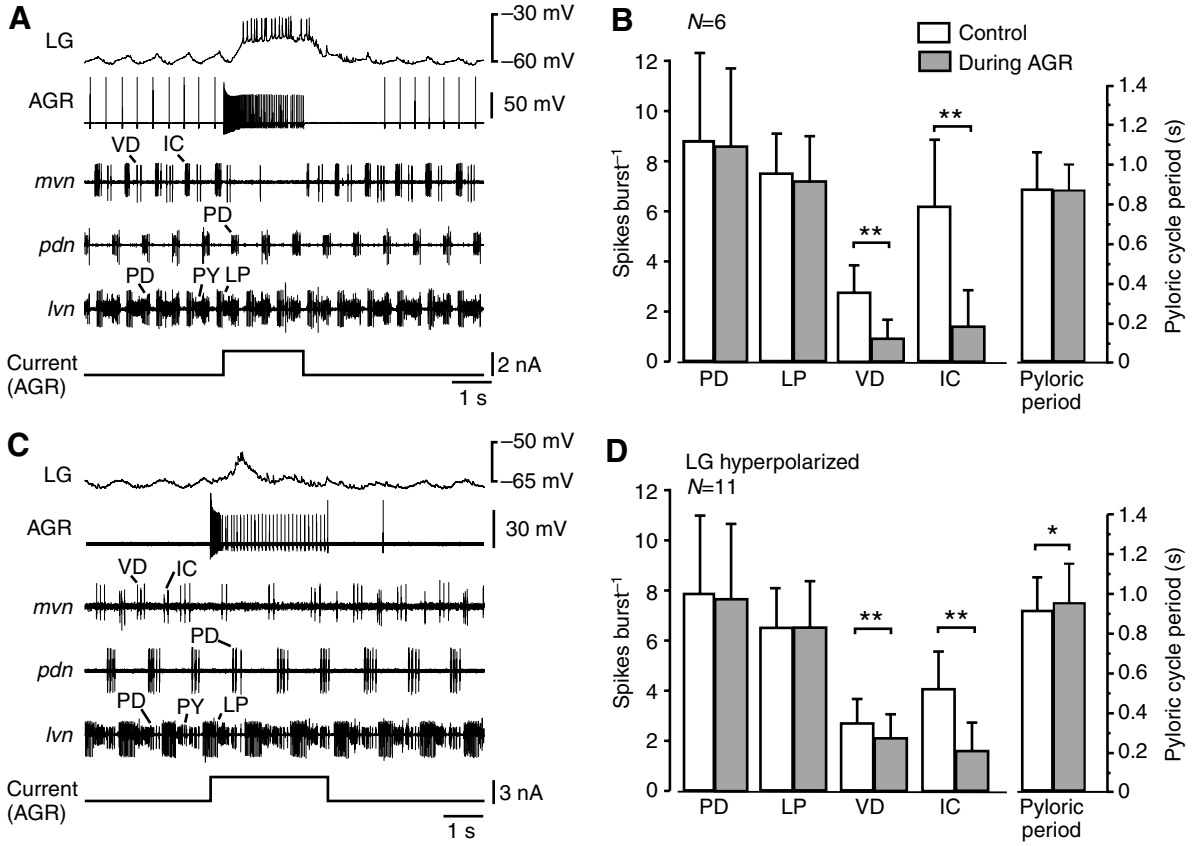

Fig. 4. AGR affects the pyloric rhythm. (A) Intracellular recordings of AGR and LG and extracellular recordings of three pyloric nerves. AGR was depolarized with current injection. While the spike activities of IC and VD were diminished during the depolarization, LG was activated by the stimulus. (B) Mean number of spikes per burst of the pyloric neurons PD, LP, VD and IC, and pyloric cycle period before (open boxes) and during AGR stimulation (filled boxes) when LG was active. $^{**}P<0.01$. (C) Same experiment as in A. Current injection was used to prevent spike activity in LG. (D) On average, IC and VD activity was diminished during AGR activity, even when LG was not active. In addition, the pyloric period increased. $^{*}P<0.05$. See text for definition of abbreviations.

mill muscles 1 (gm1) *via* the dorsal gastric nerve *dgn* and the anterior gastric nerve *agn* (Fig. 1A). The ascending axon of AGR projected to the commissural ganglia (CoGs), *via* the stomatogastric nerve *stn* and the superior oesophageal nerves (*son*s; in contrast to the lobster, in which the axon is found in the inferior oesophageal nerve *ion*). Backfills and stainings revealed no obvious arborization within the STG. In the isolated nervous system, AGR was usually tonically active with low firing frequencies (2.26±0.98 Hz; N=12). In contrast to the lobsters *H. gammarus* (Combes et al., 1997) and *P. interruptus* (Elson et al., 1994), AGR in *C. pagurus* never showed spontaneous oscillations (N>50 recordings). However, rhythmic bursts could be elicited with focal application of neuropeptide F1 (10^{-6} mol l^{-1}) to the dendritic region of AGR (N=4; data not shown). Application of F1 to the soma, by contrast, never elicited oscillations (N=6).

AGR spikes could be monitored on all nerves mentioned above (Fig. 1C). We found that AGR possessed two spike initiation zones, each of which might be responsible for the spontaneous activity. Fig. 1C demonstrates that, even within a single animal, both spike initiation zones could be active. Spikes either originated in the *agn* and travelled towards the CoGs (Fig. 1C, top) or they were elicited in the *stn* in a way that spikes travelled in two directions, towards the CoGs and towards the *agn* (Fig. 1C, bottom).

To assess the functional role of AGR in *C. pagurus*, we used a neuromuscular preparation with the gm1 muscles and their innervation left intact while extracellularly recording AGR on the *dgn* and/or the *stn*. The anterior apodemes of the gm1 muscles were fixed to the Sylgard®. We then tested the AGR response with two different approaches. (1) We applied gentle stretch to the gm1 muscles by mechanically moving the posterior ossicles to which the gm1 muscles are attached (N=5). AGR activity increased with passive stretch (Fig. 2A). Stronger stretch resulted in stronger AGR responses. (2) In preparations with spontaneous gastric mill rhythms, we monitored AGR during active contractions of the gm1 muscles (N=6). Here, the posterior ossicle was pinned down to the Sylgard® so that activity of the GM motor neurons elicited isometric muscle contractions. We found that AGR firing frequency increased when GM was active (Fig. 2B). During both isometric contraction and passive stretch of the gm1 muscles, AGR spikes originated in the dendritic region close to the gm1 muscles and were relayed towards the CoGs. Together with the fact that AGR responded to active as well as passive forces developed in the muscles, this finding suggests that AGR functions as a tension receptor of the gm1 muscles.

Intracellular recordings from the AGR soma revealed a resting potential of –60.42±5.20 mV (*N*=11). No synaptic inputs of any kind were obvious. Action potentials showed a mean amplitude of 57.36±28.10 mV (*N*=11). AGR showed strong spike frequency adaptation, when depolarized with tonic current steps into the soma (2 s duration; Fig. 3A), which contrasts with the situation in the lobsters. In steady state, AGR firing rates settled at about 20% of the maximum firing frequencies reached at the beginning of the current injection. Initial firing frequencies could reach up to 100 Hz. When negative constant-current pulses were applied, the membrane potential attained an early hyperpolarized peak and then decayed (sag) to a steady level (Fig. 3B). On termination of the pulse, the membrane response transiently overshot the resting potential such that AGR firing frequencies exceeded those obtained prior to the pulse. Both peak potential and rebound depended on the amount of the injected current (Fig. 3A,B).

Response of the pyloric circuit to AGR stimulation

As a first step to examine AGR actions on the CPGs in the STG, we characterized its influence on the pyloric motor neurons. We measured the spike activity of pyloric neurons and pyloric cycle frequency while we applied current pulses of two or more seconds into the AGR soma. Since AGR showed spike frequency adaptation, we were unable to maintain AGR firing frequencies over the time period required for measuring the different pyloric parameters in some experiments. We thus used a sequence of current pulses (250 ms duration followed by a pause of 250 ms) to prevent adaptation in these experiments.

As is obvious from the original recording in Fig. 4A, the activities of two pyloric neurons were affected. On average, the number of spikes per burst of the VD and IC neurons diminished significantly (VD, from 2.7±1.2 spikes burst^{-1} to 0.9±0.9 spikes burst^{-1} during AGR firing; IC, from 6.1± 2.7 spikes burst^{-1} to 1.3±1.5 spikes burst^{-1} when AGR was activated; *N*=6, *P*<0.01; Fig. 4B). However, not only pyloric neurons were affected by AGR stimulation, but also the gastric mill motor neuron LG (Fig. 4A, top recording; see also below). Due to its gastropyloric interactions (Bartos and Nusbaum, 1997), LG has a strong impact on pyloric activity. To assess whether VD and IC were directly affected by AGR or indirectly *via* LG actions on the pyloric circuit, we eliminated the LG effect by hyperpolarizing it with current injections into its soma to prevent it from spiking (Fig. 4C). As a result, we found that IC and VD still showed a significant change in spike activity in these conditions (IC, from 4.08±1.5 s without AGR stimulation to 1.59±1.1 s during AGR, *P*<0.01, *N*=11; VD, from 2.68±0.9 s without AGR to 2.11±0.9 s with AGR, *P*<0.01, *N*=11; Fig. 4D). Additionally, the pyloric period increased (from 0.9±0.2 s without AGR stimulation to 1.0±0.2 s during AGR stimulation; *P*<0.05, *N*=11).

The AGR actions on IC and VD appear to be entirely mediated by the actions of descending projection neurons in the CoGs, because the pyloric circuit was no longer affected (*N*=6; data not shown) when we transected the *son*s and thus also the AGR axons to the CoGs.

Response of the gastric mill circuit to AGR stimulation

As mentioned above, gastric mill neurons were affected by AGR stimulation. We characterized the response of several gastric mill neurons with intracellular recordings (*N*>6 recordings for each type of neuron). As shown in Fig. 5A, AGR excited the medial tooth protractor motor neurons, the GMs (four cells) and the protractor of the lateral teeth LG (a member

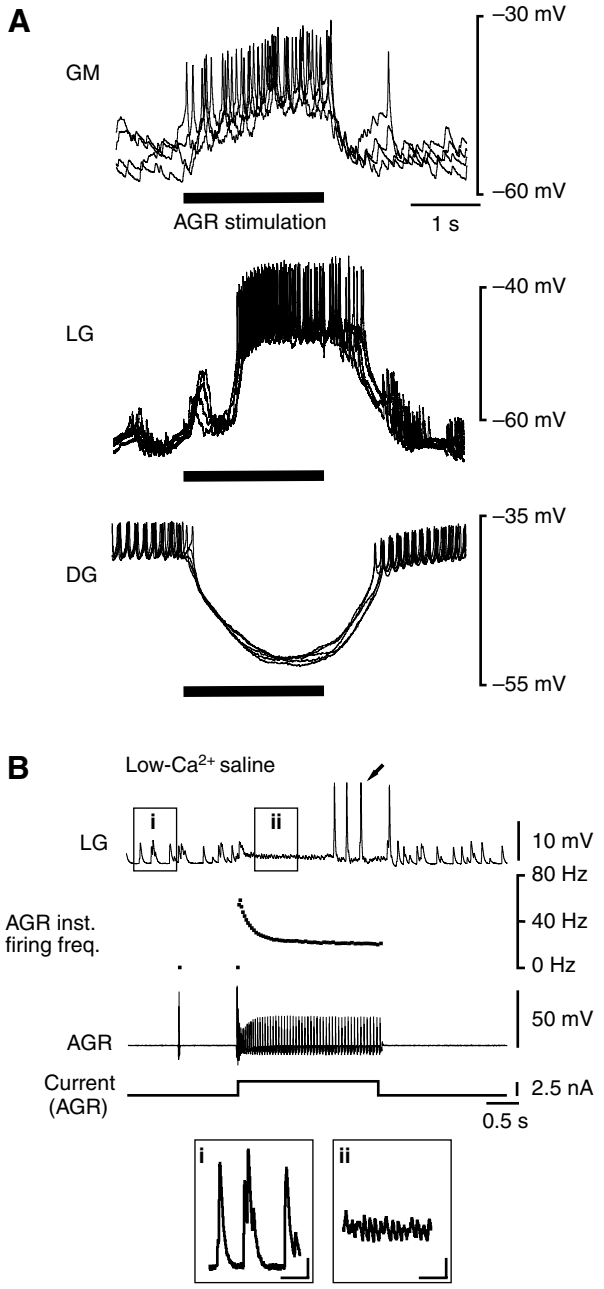

Fig. 5. Influence of AGR on gastric mill motor neurons. (A) Intracellular recordings of the gastric mill neurons GM, LG and DG. Superposition of five sweeps during AGR stimulation, triggered at the beginning of the AGR stimulus. LG and GM were excited during the AGR stimulation, DG received hyperpolarization. (B) In low-Ca^{2+}-saline, LG received at least two different types of electrical PSPs. Before and after AGR activity, large PSPs were present (i). During AGR activity, these large PSPs disappeared and small PSPs showed up (ii). During the course of the stimulation, the large PSPs reappeared and elicited action potentials (arrow). Horizontal scale bars in i and ii, 0.2 s; vertical, 1 mV). See text for definition of abbreviations.

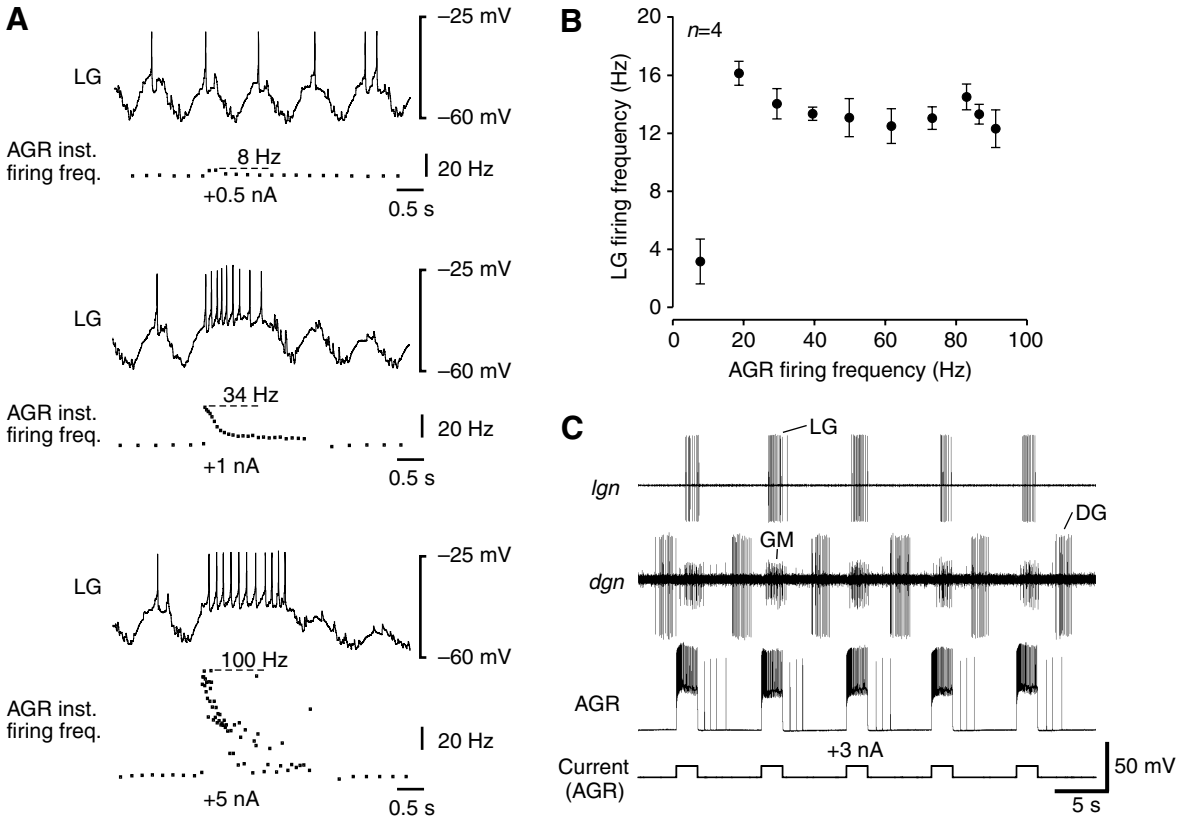

Fig. 6. LG shows no inactivation during strong AGR firing. (A) Response of LG to AGR depolarization with different currents (bottom, +5 nA; middle, +1 nA; top, +0.5 nA). AGR activity is shown as instantaneous firing frequency. (B) Plot of LG intraburst firing frequency over AGR firing frequency. (C) In preparations without spontaneous gastric mill rhythms, rhythmic AGR stimulation elicited a gastric mill rhythm which included activity of pro- (LG, GM) and retractor motor neurons (DG). See text for definition of abbreviations.

of the gastric mill CPG), while it inhibited the retractor motor neuron DG. No postsynaptic potentials time-locked to the AGR spikes were observed in either motor neuron [although discrete post-synaptic potentials (PSPs) were obvious, see below].

When high divalent saline was applied to the STG, which increases spike threshold (M. P. Nusbaum, personal communication) and thus blocked polysynaptic chemical pathways, GM and LG still received excitation and DG was still hyperpolarized during AGR stimulation (N=4; not shown). High divalent saline was bath-applied exclusively to the STG such that AGR effects on the CoGs remained unaffected. When we blocked chemical synapses in the STG with low-Ca^{2+} saline (N=4 for each neuron), the AGR excitation of GM and LG persisted (shown for LG in Fig. 5B). As expected, DG was no longer affected in low-Ca^{2+} saline. Thus, AGR either directly affected DG (and not *via* circuit interactions in the STG) and was electrically coupled to LG and GM or it acted on descending projection neurons in the CoGs, which then directly affected these neurons. The latter appears to be valid, since all effects on the gastric mill motor neurons vanished when the AGR axons to the CoGs were transected (N=6; data not shown).

In contrast to GM, which received uniform electrical PSPs throughout the duration of the AGR stimulation in low-Ca^{2+} saline (intact AGR axons), LG received two different types of PSPs (Fig. 5B). Before AGR stimulation, LG received rather large PSPs (Fig. 5Bi). At the beginning of the stimulation, these PSPs disappeared and a barrage of smaller PSPs commenced, which continued throughout the stimulus (Fig. 5Bii). Towards the end of the stimulus, the large PSPs reappeared and occasionally elicited spikes (arrow in Fig. 5B). After the end of the AGR stimulus, the small PSPs disappeared and the larger ones resumed their initial frequency. While we did not further investigate the origin of these PSPs, it is reasonable to assume that they were elicited by descending projection neurons. Thus, the AGR effect on LG was mediated *via* the actions of at least two different projection neurons.

In the lobster, AGR actions on the gastric mill circuit depended on AGR firing frequency (Combes et al., 1999; Elson et al., 1994; Simmers and Moulins, 1988a). While low AGR firing frequencies excited the protractor motor neurons, high firing frequencies failed to excite them. By contrast, we found that in *C. pagurus* different AGR firing frequencies had similar effects on the gastric mill motor neurons, at least qualitatively (Fig. 6A). We verified this finding with 2 s current injections into the AGR soma (N=7). Even when the initial firing frequency at the beginning of the AGR depolarization was close to 100 Hz, LG and GMs were still excited by the stimulus and DG received inhibition. This phenomenon is exemplified for a single animal in Fig. 6B, in which we plotted the response of the LG motor neurons over the mean AGR firing frequency during the stimulus. Apparently, there was no switch from the

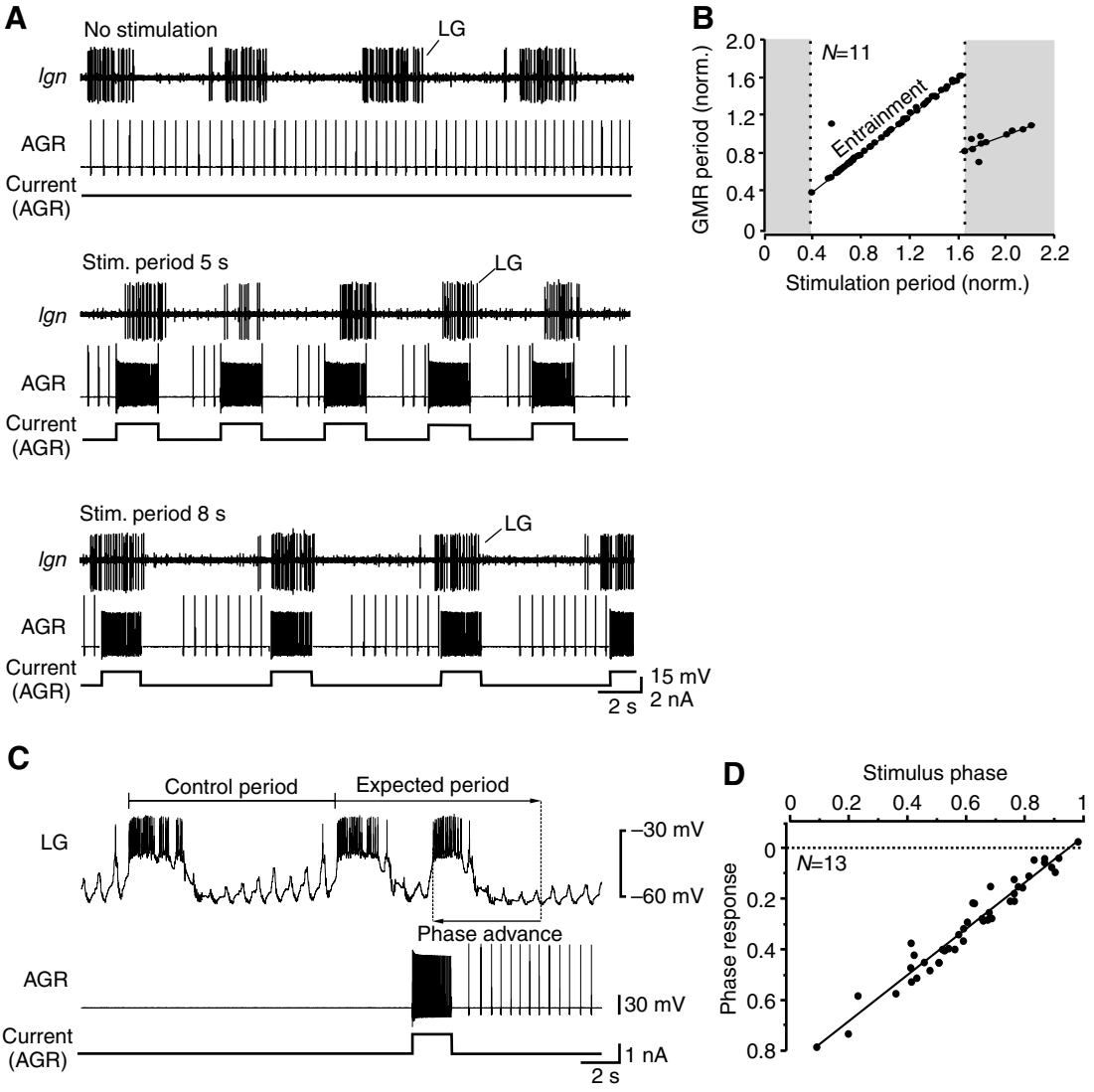

Fig. 7. Influence of AGR on spontaneous gastric mill rhythms. (A) Entrainment of a gastric mill rhythm with rhythmic activation of AGR. Original recordings of *lgn* and intracellular recording of AGR. Top: control, AGR was not stimulated. Middle: AGR was stimulated with a period of 5 s. The gastric mill rhythm was entrained to the stimulus. Bottom: stimulation of AGR with a period longer than control (8 s). The period of the rhythm corresponded to that of the stimulation. (B) Entrainment of the gastric mill rhythm. Mean of N=11 animals. The period of the rhythm is plotted over stimulation period. Both parameters are normalized to the period of the spontaneous rhythm (control). Linear regression between 0.4 and 1.6 stimulation period, R^2=0.99. GMR, gastric mill rhythm. (C) Response of LG to a single burst of AGR during a spontaneous gastric mill rhythm. The AGR burst shortened the expected cycle period (phase advance). (D) Mean phase response curve of LG. AGR stimulation was capable of resetting the rhythm at any phase of the cycle. Linear regression, R^2=0.95. See text for definition of abbreviations

active state to the inactive state of the LG neuron. However, LG firing frequency did not increase with stronger AGR activity.

AGR responds to an increase of the tension of the gastric mill muscle gm1 (Fig. 1A) (Simmers and Moulins, 1988a; Simmers and Moulins, 1988b). Tension increases with the activity of the gastric mill motor neurons driving the muscles. AGR will thus be activated according to the prevailing gastric mill rhythm, which usually shows periods of a few seconds to more than 10 s (Stein et al., 2006). To test the effects of AGR on the gastric mill rhythm, we thus used current injections into the AGR soma to rhythmically activate it with a burst duration of 2 s and a period of 10 s. To start with, we applied current injections in preparations without spontaneous gastric mill rhythms (N=28). In all experiments, a gastric mill rhythm was elicited that included bursting of both the pro- and retractor motor neurons (Fig. 6C). In these experiments, all protractor motor neurons (GMs and LG) were active in time with the AGR stimulus train.

In preparations with spontaneously active gastric mill rhythm (N=12), and thus in a situation in which AGR would likely be active in intact animals, rhythmic AGR stimulation entrained the rhythm. In the experiment shown in Fig. 7A, the period of the spontaneous gastric mill rhythm was 6.4±0.4 s (n=10). When AGR stimulus trains with a period of 5 s were applied, the period of the gastric mill rhythm sped up to a period of 5.0±0.3 s (n=10). By contrast, when the stimulation period was slower (8 s) than the control period of the gastric mill rhythm,

the rhythm slowed down and now showed a period of 7.9±0.7 s (n=10). Stable phase-locking was attained after three or fewer transient cycles, and after the end of AGR stimulation the cycle period immediately reverted to its free-running value. Fig. 7B summarizes the results of N=11 experiments. Here, we plotted the period of the gastric mill rhythm over stimulation period. Both parameters were normalized to the period of the spontaneous gastric mill rhythm in order to compare animals with varying control periods. The plot shows that the rhythm could be entrained between 0.4 and 1.6 normalized stimulation periods, which indicates that rhythmic AGR stimulation could decrease or increase the period of rhythm up to 60% of the original period (slope 0.99, N=11, n=55, R^2=0.99, P<0.01). With shorter or longer stimulus periods, we either observed no entrainment or two gastric mill cycles per stimulus cycle (Fig. 7B, right-hand grey box), respectively.

As is obvious from the original recording in Fig. 7A (bottom), the onset of the LG bursts could be prior to the onset of the AGR activity during entrainment. This resulted from the rhythmic nature of the AGR stimulation. To further characterize the impact of AGR on the gastric mill CPG, we thus also tested the response of the gastric mill rhythm to single AGR bursts, applied at different phases of the rhythm (Fig. 7C). The resulting phase–response curve (Fig. 7D) revealed a linear relationship between stimulus phase and the phase response of the rhythm with a slope of 0.92 (N=13, n=45, R^2=0.95, P<0.01). A slope of 1.0 would indicate a strong reset of the rhythm (type 0 reset) (Winfree, 2001; Izhikevich, 2006). Our results thus show that AGR stimulation was capable of resetting the gastric mill rhythm at any phase of the rhythm.

Discussion

Projection pattern and intrinsic properties of the sensory neuron AGR

We investigated the sensory neuron AGR in the isolated stomatogastric nervous system. AGR had previously been characterized in two different crustacean species, the lobster *Homarus gammarus* (Combes et al., 1999; Combes et al., 1995; Combes et al., 1997; Simmers and Moulins, 1988a; Simmers and Moulins, 1988b) and the spiny lobster *Panulirus interruptus* (Elson et al., 1994). We now aim at expanding our knowledge about this sensory neuron by examining it in a third crustacean species, *Cancer pagurus*. Two main goals motivated this study. (1) So far, only AGR actions on the gastric mill circuit have been investigated. For a functional processing of food, however, the movement of the teeth needs to be coordinated with the pyloric filter apparatus. We thus examined the AGR influence on the pyloric rhythm with gastric mill rhythm present and with inhibited gastric mill activity. (2) Some physiological properties of AGR and some of its effects on the gastric mill rhythm appear to differ between both lobster species, yet its function is similar (to measure tension of the protractor muscles gm1). We wanted to compare AGR properties and function in the crab with those in the lobster to identify features important for all species investigated. This work also provides an initial framework for future studies to determine how AGR affects the STG circuits in the crab. All AGR effects appear to be mediated *via* CoG projection neurons. Since these neurons are well known in the crab (reviewed in Nusbaum and Beenhakker, 2002), this system is ideally suited for studying the mechanisms underlying AGR actions.

AGR in the crab shows several similarities to AGR in the lobsters. It occurs as a single bipolar soma at the posterior end of the STG (Fig. 1) and responds to an increase in tension of the gm1 muscles (Fig. 2). It thus acts as a muscle tendon organ. As in the lobsters, AGR innervates the gm1 muscles and the CoGs; however, *via* different routes. In *C. pagurus* (Fig. 1A), and also in a close relative, *C. borealis* (M. P. Nusbaum and C.R.S., unpublished observation), the AGR axon projects through the *dgn* and *agn* towards the gm1 muscle (instead of the *dvn* and *agn* as in the lobster). Also, as in *C. borealis*, AGR innervates the CoGs *via* the *son*s (Fig. 1A).

One striking feature of AGR in the crab is the strong spike frequency adaptation when depolarizing current is applied into the soma (Fig. 3A). This tendency of the membrane potential to move towards the resting potential was either not present in lobsters or only weakly affected AGR firing rate (Elson et al., 1994; Simmers and Moulins, 1988b). By contrast, in our experiments, we were unable to maintain firing frequencies for an extended time period. In fact, it proved to be necessary in some experiments to use repetitive current pulses to prevent the attenuation of AGR firing frequencies. The success of this procedure in turn suggests that spike frequency adaptation may be mediated by a voltage-dependent effect because adaptation was less effective when the membrane potential returned to values close to the resting potential in between two current pulses. After the end of current injection, the membrane potential temporarily dropped below resting potential and spiking usually stopped for a few seconds.

When AGR was hyperpolarized by tonic current injection, the membrane potential attained an early peak and then decayed to a steady level (Fig. 3B). This ‘sag’ is common in many STG neurons and is often elicited by a hyperpolarization-activated and voltage-dependent current (inward rectifier, I_h) (Buchholtz et al., 1992). In sensory neurons, however, such a response to hyperpolarization appears rather unusual, especially in the sense that AGR does not receive any obvious synaptic input. In addition, we observed a post-inhibitory rebound after the release from inhibition such that the membrane response transiently overshot the resting potential (Fig. 3B). Consequently, AGR firing frequencies exceeded those obtained prior to current injection.

Spike frequency adaptation, sag and post-inhibitory rebound may serve different functions in the perception of muscle tension. Since AGR appears to be a conditional oscillator, one obvious interpretation is that these properties support the membrane oscillations obtained when neuropeptide F1 is present at the dendritic region. However, such membrane properties are often under neuromodulatory control and are either activated or amplified in the presence of suitable modulators (Saideman et al., 2007). It thus remains unclear why the observed membrane properties are so potently present in non-rhythmic preparations (in normal saline). It is conceivable, however, that voltage-dependent membrane properties also support the normal functioning of the receptor in non-rhythmic conditions. If the initial high firing frequencies and their quick adaptation are functionally relevant (see below), sag and post-

inhibitory rebound may support a quick return to the resting potential (and thus help to prepare AGR for the detection of the next muscle tension increase) by compensating the hyperpolarization after the end of strong AGR activity.

Effects on the pyloric and gastric circuit

The impact of AGR on the pyloric rhythm has not been previously described. Our results show that AGR diminished the spike activities of two pyloric neurons, IC and VD. Both are follower neurons and do not directly interfere with pattern generation in the pyloric circuit. Nevertheless, the pyloric cycle period increased during AGR stimulation. All observed effects apparently were not based on gastropyloric interactions since we obtained similar results when blocking spike activity in the gastric mill neuron LG by applying tonic hyperpolarizing current. LG strongly affects pyloric pattern generation *via* the presynaptic inhibition it exerts on the axon terminals of an excitatory descending projection neuron (Bartos and Nusbaum, 1997). Since all effects on the pyloric rhythm disappeared when AGR axons to the CoGs were severed, we conclude that the inhibitory effect on the pyloric neurons was mediated *via* descending projection neurons.

The actions of AGR on the gastric mill circuit were much more pronounced than those on the pyloric circuit. The phase–response curve (Fig. 7D) shows that AGR was capable of resetting the gastric mill rhythm independently of stimulus phase. Phase–response curves show the change in oscillator period elicited by inputs occurring at different phases in the rhythm (Prinz et al., 2003; Wolf and Pearson, 1988) and thus are a solid way of confirming the functional significance of a discrete input to an oscillatory system (Abramovich-Sivan and Akselrod, 1998). As a result of AGR resetting capabilities, rhythmic AGR stimulation entrained the rhythm (Fig. 7A). Entrainment of the gastric mill rhythm has also been shown in *P. interruptus* (Elson et al., 1994) but has never been studied systematically. We here show that AGR entrained the rhythm over a broad range of cycle periods and thus has a profound impact on gastric mill pattern generation. The period of ongoing rhythms could be decreased or increased up to 60% (Fig. 7B).

Functional aspects of AGR response

In *H. gammarus*, AGR participates in a complex control of forces exerted during the gm1 muscle powerstroke. This is exemplified by the fact that the gastric mill neurons receive excitation during moderate AGR firing frequencies, while this excitation is either absent (Simmers and Moulins, 1988b) or superimposed by inhibition (Elson et al., 1994) during higher firing frequencies. This is due to the nonlinear intrinsic membrane properties of an interneuron involved in mediating AGR effects on the gastric mill neurons (Simmers and Moulins, 1988b). As a consequence, low AGR firing frequencies synchronize the movements of medial and lateral teeth, while strong AGR firing elicits alternating movements of the teeth (Combes et al., 1999). However, our results suggest that the sign of the response (excitation/inhibition) of gastric mill and pyloric neurons is independent of AGR firing frequency (Fig. 6B). This finding stresses the relevance of the phase–response curve, which is then not only valid for moderate but also for strong AGR firing, and it indicates that *C. pagurus* may not need a whole range of influences from AGR to the gastric mill network. It is conceivable, therefore, that AGR has built-in buffering mechanisms preventing it from going to high activity rates (i.e. spike-rate adaptation) or from being shut down (i.e. sag). Interestingly, however, LG received two types of excitatory (electrical) synaptic inputs (Fig. 5B), one of which was initially weakened and then reappeared (Fig. 5B), probably due to the spike frequency adaptation of AGR. Such delayed recurrence may lead to a delayed onset of the LG burst and thus to a different phasing of the gastric mill neurons. In this way the involvement of interneuronal pathways in combination with intrinsic properties of AGR could functionally replace the nonlinear membrane properties of the interneuronal pathway involved in *H. gammarus*.

In general, this study shows that homologous proprioceptors in different, but related, species regulate motor pattern *via* different mechanisms. It provides an initial framework for future studies to examine the mechanisms of sensory processing and common principles of sensorimotor integration in the stomatogastric nervous system.

List of abbreviations

agn	anterior gastric nerve
AGR	anterior gastric receptor neuron
CoG	commissural ganglion
DG	dorsal gastric neuron
dgn	dorsal gastric nerve
GM	gastric mill neuron
IC	inferior cardiac neuron
ion	inferior oesophageal nerve
LG	lateral gastric neuron
lgn	lateral gastric nerve
LP	lateral pyloric neuron
lvn	lateral ventricular nerve
mvn	medial ventricular nerve
OG	oesophageal ganglion
PD	pyloric dilator neuron
pdn	pyloric dilator nerve
PSP	postsynaptic potential
son	superior oesophageal nerve
STG	stomatogastric ganglion
stn	stomatogastric nerve
STNS	stomatogastric nervous system
VD	ventricular dilator neuron

This work was supported by DFG STE 937/2-1 and STE 937/2-2. We would like to thank Harald Wolf and Ursula Seifert for their support and helpful comments on the paper.

References

Abramovich-Sivan, S. and Akselrod, S. (1998). A single pacemaker cell model based on the phase response curve. *Biol. Cybern.* **79**, 67-76.

Bartos, M. and Nusbaum, M. P. (1997). Intercircuit control of motor pattern modulation by presynaptic inhibition. *J. Neurosci.* **17**, 2247-2256.

Beenhakker, M. P. and Nusbaum, M. P. (2004). Mechanosensory activation of a motor circuit by coactivation of two projection neurons. *J. Neurosci.* **24**, 6741-6750.

Blitz, D. M. and Nusbaum, M. P. (1997). Motor pattern selection via inhibition of parallel pathways. *J. Neurosci.* **17**, 4965-4975.

Blitz, D. M. and Nusbaum, M. P. (1999). Distinct functions for cotransmitters mediating motor pattern selection. *J. Neurosci.* **19**, 6774-6783.

Buchholtz, F., Golowasch, J., Epstein, I. R. and Marder, E. (1992).

Mathematical model of an identified stomatogastric ganglion neuron. *J. Neurophysiol.* **67**, 332-340.

Büschges, A. (2005). Sensory control and organization of neural networks mediating coordination of multisegmental organs for locomotion. *J. Neurophysiol.* **93**, 1127-1135.

Coleman, M. J., Nusbaum, M. P., Cournil, I. and Claiborne, B. J. (1992). Distribution of modulatory inputs to the stomatogastric ganglion of the crab, Cancer borealis. *J. Comp. Neurol.* **325**, 581-594.

Combes, D., Simmers, J., Nonnotte, L. and Moulins, M. (1993). Tetrodotoxin-sensitive dendritic spiking and control of axonal firing in a lobster mechanoreceptor neurone. *J. Physiol.* **460**, 581-602.

Combes, D., Simmers, J. and Moulins, M. (1995). Structural and functional characterization of a muscle tendon proprioceptor in lobster. *J. Comp. Neurol.* **363**, 221-234.

Combes, D., Simmers, J. and Moulins, M. (1997). Conditional dendritic oscillators in a lobster mechanoreceptor neurone. *J. Physiol.* **499**, 161-177.

Combes, D., Meyrand, P. and Simmers, J. (1999). Dynamic restructuring of a rhythmic motor program by a single mechanoreceptor neuron in lobster. *J. Neurosci.* **19**, 3620-3628.

Cropper, E. C., Evans, C. G., Jing, J., Klein, A., Proekt, A., Romero, A. and Rosen, S. C. (2004). Regulation of afferent transmission in the feeding circuitry of Aplysia. *Acta Biol. Hung.* **55**, 211-220.

Elson, R. C., Panchin, Y. V., Arshavsky, Y. I. and Selverston, A. I. (1994). Multiple effects of an identified proprioceptor upon gastric pattern generation in spiny lobsters. *J. Comp. Physiol. A* **174**, 317-329.

Hartline, D. K. and Maynard, D. M. (1975). Motor patterns in the stomatogastric ganglion of the lobster *Panulirus argus*. *J. Exp. Biol.* **62**, 405-420.

Heinzel, H. G., Weimann, J. M. and Marder, E. (1993). The behavioral repertoire of the gastric mill in the crab, *Cancer pagurus*: an *in situ* endoscopic and electrophysiological examination. *J. Neurosci.* **13**, 1793-1803.

Izhikevich, E. M. (2006). *Dynamical Systems in Neuroscience – The Geometry of Excitability and Bursting*. Cambridge, MA: MIT Press.

Larimer, J. L. and Kennedy, D. (1966). Visceral afferent signals in the crayfish stomatogastric ganglion. *J. Exp. Biol.* **44**, 345-354.

Marder, E. and Bucher, D. (2001). Central pattern generators and the control of rhythmic movements. *Curr. Biol.* **11**, R986-R996.

Maynard, D. M. and Dando, M. R. (1974). The structure of the stomatogastric neuromuscular system in *Callinectes sapidus*, *Homarus americanus* and *Panulirus argus* (Decapoda Crustacea). *Philos. Trans. R. Soc. Lond. B Biol. Sci.* **268**, 161-220.

Norris, B. J., Coleman, M. J. and Nusbaum, M. P. (1994). Recruitment of a projection neuron determines gastric mill motor pattern selection in the stomatogastric nervous system of the crab, *Cancer borealis*. *J. Neurophysiol.* **72**, 1451-1463.

Nusbaum, M. P. and Beenhakker, M. P. (2002). A small-systems approach to motor pattern generation. *Nature* **417**, 343-350.

Perrins, R., Walford, A. and Roberts, A. (2002). Sensory activation and role of inhibitory reticulospinal neurons that stop swimming in hatchling frog tadpoles. *J. Neurosci.* **22**, 4229-4240.

Prinz, A. A., Thirumalai, V. and Marder, E. (2003). The functional consequences of changes in the strength and duration of synaptic inputs to oscillatory neurons. *J. Neurosci.* **23**, 943-954.

Saideman, S. R., Ma, M., Kutz-Naber, K. K., Cook, A., Torfs, P., Schoofs, L., Li, L. and Nusbaum, M. P. (2007). Modulation of rhythmic motor activity by pyrokinin peptides. *J. Neurophysiol.* **97**, 579-595.

Selverston, A. I. and Moulins, M. (1987). *The Crustacean Stomatogastric System*. Berlin, Heidelberg, New York, London, Paris, Tokyo: Springer Verlag.

Simmers, J. and Moulins, M. (1988a). A disynaptic sensorimotor pathway in the lobster stomatogastric system. *J. Neurophysiol.* **59**, 740-756.

Simmers, J. and Moulins, M. (1988b). Nonlinear interneuronal properties underlie integrative flexibility in a lobster disynaptic sensorimotor pathway. *J. Neurophysiol.* **59**, 757-777.

Stein, W., Eberle, C. C. and Hedrich, U. B. S. (2005). Motor pattern selection by nitric oxide in the stomatogastric nervous system of the crab. *Eur. J. Neurosci.* **21**, 2767-2781.

Stein, W., Smarandache, C. R., Nickmann, M. and Hedrich, U. B. (2006). Functional consequences of activity-dependent synaptic enhancement at a crustacean neuromuscular junction. *J. Exp. Biol.* **209**, 1285-1300.

Weimann, J. M., Meyrand, P. and Marder, E. (1991). Neurons that form multiple pattern generators: identification and multiple activity patterns of gastric/pyloric neurons in the crab stomatogastric system. *J. Neurophysiol.* **65**, 111-122.

Winfree, A. T. (2001). *The Geometry of Biological Time*. New York: Springer.

Wolf, H. and Pearson, K. G. (1988). Proprioceptive input patterns elevator activity in the locust flight system. *J. Neurophysiol.* **59**, 1831-1853.

Wolf, H., Bassler, U., Spiess, R. and Kittmann, R. (2001). The femur–tibia control system in a proscopiid (Caelifera, Orthoptera): a test for assumptions on the functional basis and evolution of twig mimesis in stick insects. *J. Exp. Biol.* **204**, 3815-3828.